Scripta Materialia 202 (2021) 114009

Contents lists available at ScienceDirect

Scripta Materialia

journal homepage: www.elsevier.com/locate/scriptamat

First-principles Calculations of Bulk and Interfacial Thermodynamic Properties of the T_1 phase in Al-Cu-Li alloys

Beomjin Na[a], Bi-Cheng Zhou[b], C. Wolverton[c], Kyoungdoc Kim[a,*]

[a] Department of Materials Science and Engineering, Inha University, Incheon 22212, Republic of Korea
[b] Department of Materials Science and Engineering, University of Virginia, Charlottesville, VA 22904, United States
[c] Department of Materials Science and Engineering, Northwestern University, Evanston, IL 60208, United States

ARTICLE INFO

Article history:
Received 18 February 2021
Revised 3 May 2021
Accepted 17 May 2021
Available online 3 June 2021

Keywords:
Aluminum alloys
Precipitation hardening
Interfacial energy
First-principles calculation
Density-functional theory

ABSTRACT

We recently proposed a new, low-energy atomic structure of the Al_2CuLi (T_1) phase using first-principles calculations based on density functional theory [*Acta Mater. 145 (2018) 337-346*]. Here, we refine the Li positions in the proposed T_1 structure and find that the T_1 phase has a tie-line with Al at finite-temperature by vibrational entropic stabilization on the Gibbs triangle of the ternary Al-Cu-Li system. We also derive a low-energy T_1/Al coherent interfacial structure and find that Ag and Mg solutes are predicted to segregate to the coherent interface, which is in agreement with recent experimental observations by atom probe tomography.

Precipitation-strengthened alloys such as those based on aluminum are widely used in transportation. Aluminum-lithium (Al-Li) alloys are of great interest in aerospace applications where superior specific strength (high strength/low density) is required [1,2]. This is because lithium additions reduce density (~3% decrease per every weight percent) and increase elastic modulus (~6% increase per every weight percent) [3]. Cu additions further increase the strength of aluminum alloys in the Al-Cu-Li system in the limit of Li content (lower than 2 wt.%) due to the long-term embrittlement [3]. In the ternary Al-Cu-Li system, the main strengthening precipitate is a hexagonal Al_2CuLi (T_1), which forms nanometer-sized thin plates on the $\{111\}_{Al}$ planes when embedded in Al matrix [4].

The crystal structure of the T_1 phase has been studied extensively by various experimental groups [5–9]. However, these studies contain several distinct proposals for the crystal structure of T_1. In order to reconcile the discrepancies in these reports, and to determine the thermodynamically stable crystal structure of the T_1 phase, we previously performed first-principles calculations based on Density Functional Theory (DFT) using crystal structure information in experiments [10]. According to the experimental information, there are two compositional degrees of freedom in the T_1 structure: 1) Li partial occupancy in its position; 2) Al-Cu mixing in two-dimensional configurations. In the previous study, we first investigated various configurations of the half-occupied Li layers under an assumption of fully occupied Al or Cu in the Al-Cu mixed layer. We then derived a lowest-energy ordered configuration of Al-Cu using cluster expansion methods. Based on our computations, we proposed a new structure of the T_1 phase, which has DFT energy lower than all of the experimentally proposed crystal structures. And, we found the DFT energy of the new proposed structural model places it on the convex hull, and hence this compound is stable (at T=0K) in the Al-Cu-Li ternary system. However, there are still some unanswered questions about the structure and phase stability of the T_1 phase: There is a discrepancy of the Li position between experiment [7] and computation [10]. In addition, the DFT-energy of the predicted T_1 phase structure does not have a tie-line with the Al matrix at 0K in ternary Al-Cu-Li system, which is seemingly inconsistent with the experimental observation of two-phase Al+T_1 microstructure.

The precipitate/matrix interfacial structure and energy are important thermodynamic parameters in designing high strengthened alloys. For example, the interfacial energy determines the height of energy barrier for nucleation, number density, morphology, and the size distribution of the precipitates [11]. The solute-interface interaction is also very important in optimizing the microstructure of T_1 precipitates. This is because coarsening of the precipitates can be controlled by solute segregations at interface. Gault et al. [12] found that Ag and Mg solutes do not segregate at the interface, but instead are partitioned inside the T_1 phase, as identified through Atom Probe Tomography (APT). Using the same APT

* Corresponding author.
E-mail address: kkim@inha.ac.kr (K. Kim).

https://doi.org/10.1016/j.scriptamat.2021.114009
1359-6462/

method, however, Ag and Mg have been observed to segregate to the T_1/Al interface by Araullo-Peters et al. [13] and Kang et al. [14]. Araullo-Peters et al. argued that the interfacial segregation cannot be observed when the atom probe probing direction is not perpendicular to the T_1 precipitates [13].

Here, we use first-principles calculations to determine the answers to some of the outstanding questions described above. We explore the detailed Li position in the stable T_1 structure. And we investigated finite-temperature effects (i.e., vibrational entropic contributions) to the thermodynamic stability of the T_1 phase to resolve the discrepancy between experiment and computation regarding the stability of two-phase Al+T_1. We also derived the low-energy interfacial structure of the coherent T_1/Al interface and predicted solute segregation behavior to resolve the contradictory of interface-related observations in the literature. The interfacial structure and energy determined here will be useful thermodynamic parameters to future phase-field modeling of microstructure evolution.

We performed first-principles calculations using the Vienna Ab initio Simulation Package (VASP) [15] and projector-augmented wave potentials [16]. We utilized the PBE parameterization of the generalized gradient approximation (GGA-PBE) [17] for all calculations. We relaxed all the cell-internal and cell-external degrees of freedom at an energy cutoff of 520 eV. Gamma-centered k-point meshes were constructed to achieve at least 9,000 k-points per reciprocal atom, giving the convergence of formation energy within 1meV/atom. The interfacial energy and solute segregation energy were converged within 10% and 10meV/solute atom with respect to the supercell sizes used.

Calculations of bulk energetics, interfacial stability, and solute segregation energy at the coherent T_1/Al interface were performed. First of all, we computed formation energy of compounds in Al-Cu-Li ternary system when in equilibrium with the Al matrix to compare the relative thermodynamic bulk stability at 0K. The key quantity for this calculation is the formation energy *per solute atom* [10]

$$\Delta H^{eq}(\mathrm{Al_aCu_bLi_c}) = \frac{E(\mathrm{Al_aCu_bLi_c}) - [x_A E^{eq}(\mathrm{Al}) + x_B E^{eq}(\mathrm{Cu}) + x_C E^{eq}(\mathrm{Li})]}{x_B + x_C} \tag{1}$$

where $\Delta H^{eq}(\mathrm{Al_aCu_bLi_c})$ is the equilibrium formation energy (eV/solute) of a compound relative to the pure components, Al, Cu, and Li. $E(\mathrm{Al_aCu_bLi_c})$ is the energy of the compound. $E^{eq}(\mathrm{Al})$, $E^{eq}(\mathrm{Cu})$ and $E^{eq}(\mathrm{Li})$ are the energies of the pure components from first-principles calculations. We also computed the vibrational entropies of two previously proposed T_1 structures ($Al_6Cu_4Li_3$, $Al_{13}Cu_7Li_6$) and other phases in the Al-Cu-Li system in order to include the vibrational contribution to the free energy. We use the Phonopy [18] for phonon calculations, which is based on the harmonic approximation. The thermodynamic stability of the T_1/Al interfaces was investigated based on interfacial energy calculations at 0K. We recently described how to compute interfacial energy based on the chemical potentials of pure elements in multi-component systems where the periodic boundary condition varies with the supercell size in DFT calculations [19]. The interfacial energy determined from a supercell containing the interface and a decomposition of the supercell formation energy into strain and interfacial contributions [20,21]

$$\Delta E_f = \delta E_{cs\ (Al,T_1)} + \frac{2\sigma A}{N} \tag{2}$$

where $\Delta E_f = [(x_A\mu_{Al} + x_A\mu_{Cu} + x_A\mu_{Li})/N]$ is the formation energy per atom relative to the chemical potentials (μ_{Al}, μ_{Cu}, μ_{Li}) of Al, Cu, Li. $\delta E_{cs\ (\alpha,\theta')}$ is the coherency strain per atom caused by the lattice mismatch between T_1 and Al. N is the total number of atoms in the super cell, and σ and A are the interfacial energy and area, respectively. We can obtain the interfacial energy by computing the energies of supercells of various sizes and extracting the slope of ΔE_f vs. $1/N$ in Eq. (2). For the chemical potentials of Al, Cu, and Li, we solved the following equations based on three reference (i.e., stable) phases, Al, Al_2Cu (θ'), and T_1 on the calculated convex hull [10] and in experiment [13]

$$\begin{aligned} &\mu_{Al} = E_{FCC\ Al} \\ &2\mu_{Al} + \mu_{Cu} = E_{\theta'(Al_2Cu)} \\ &6\mu_{Al} + 4\mu_{Cu} + 3\mu_{Li} = E_{T_1} \end{aligned} \tag{3}$$

The interfacial energy difference is within 20mJ/m^2 depending on reference phases (e.g., Al+$Al_3Li(\delta')$+T_1 vs. Al+$AlLi(\delta)$+T_1). Solute-interface interactions were analyzed by solute segregation energy (eV/solute atom). The segregation energy is defined as the total energy difference as a function of solute atom positions with respect to the interface in a cell. The following formula, for example, is how to compute Ag solute segregation energy at interface.

$$\Delta E_{seg} = E(Ag \rightarrow X) - E(Ag \rightarrow Al_b) + \mu_X - \mu_{Al} \tag{4}$$

Here, $E(Ag \rightarrow \mathrm{X}) - E(Ag \rightarrow \mathrm{Al_b})$ represents the total energy difference as a function of Ag solute position across an interface. The X indicates the sublattice sites near interface. For example, Al_i refers the Al plane adjacent to the interface; $T1_i^{Al}$, $T1_i^{Li}$, and $T1_{i-1}^{Cu}$ represent the lattice planes within the precipitate near interface; and Al_b refers to a bulk-like plane in the Al matrix. When a solute is located in Cu or Li sublattice sites of T_1 precipitate, the chemical potentials, $\mu_X - \mu_{Al}$ in Eq. (4), can compensate for a different number of atoms between the two supercells (first and second terms on the right side in Eq. (4)). We adopt a sign convention such that sites having $\Delta E_{seg} < 0$ in Eq. (4) are energetically favorable for solute segregation at interface relative to solid solutions in Al matrix.

Recently, we proposed [10] the new low-energy structures ($Al_6Cu_4Li_3$, $Al_{13}Cu_7Li_6$) of the T_1 phase using first-principles density functional theory calculations combined with cluster expansion methods. The proposed $T_1(Al_6Cu_4Li_3)$ phase is energetically stable on the calculated convex hull of the Al-Cu-Li system at 0K. Previously, we investigated various configurations of the Li layers in a T_1 bulk structure under an assumption of fully occupied Al or Cu in the mixed layer. We first defined these Li orderings, and subsequently explored Al-Cu configurations using first-principles calculations with cluster expansion methods. We found that the Li atoms are energetically favorable when located on the flat plane along the z-fractional coordinate, $(111)_{Al}$, in the T_1 bulk structure [10]. Since the Li position in the bulk T_1 structure deviates the flat plane experimentally [7], we further investigated ordering of Al-Li positions in a DFT-predicted $T_1(Al_6Cu_4Li_3)$ structure to ascertain how the ordered Al/Cu layers impact on the Al-Li configurations.

Fig. 1(a) represents the crystal structure of the T_1 phase ($Al_6Cu_4Li_3$) including the lowest-energy ordering found for the Al-Cu layers. A search was done for the lowest configurations of Al-Li layers in the structure depicted in in Fig. 1(b). We confirmed that the new Li position induces a lowering of energy by 0.16 meV/atom, and the corrected Li positions along the z-fractional coordinate, $(111)_{Al}$, are 0.956 and 0.044 of Li (2) instead of 0 in Table 5 of our previous study [10] .

The DFT-predicted T_1 phase is stable on the calculated convex hull of the Al-Cu-Li system [10], however, it does not have a tie-line with Al, inconsistent with the experimental phase diagram [10] as shown in Fig. 2(a). To resolve this problem, we performed finite-temperature stability analysis of T_1 in this work. The configurational entropic stabilization due to the mixing of Al-Cu layers is not large enough to make a tie-line between T_1 and Al [10]. Thus, we investigated vibrational entropic contribu-

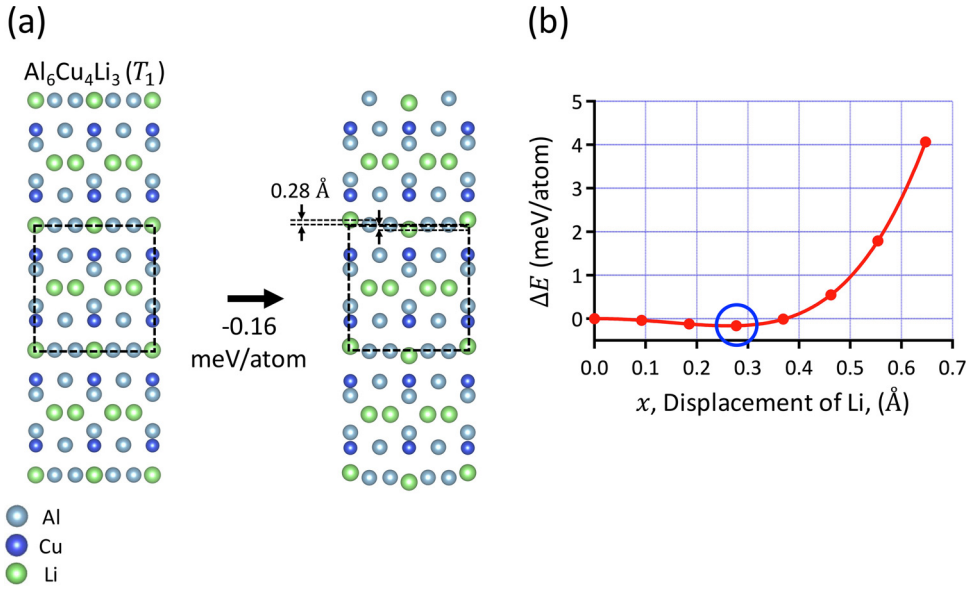

Fig. 1. (a) (Left) The DFT-predicted structure of the T_1 phase, $Al_6Cu_4Li_3$, stable on the calculated convex hull in ternary Al-Cu-Li [10] (Right) The Li position is corrected with a displacement of 0.28 Å along the interfacial normal direction, $(111)_{Al}$, in this work (b) Total energy variation as a function of displacement of Li along the $(111)_{Al}$. The calculation represents that the displacement of 0.28 Å is a lowest-energy state.

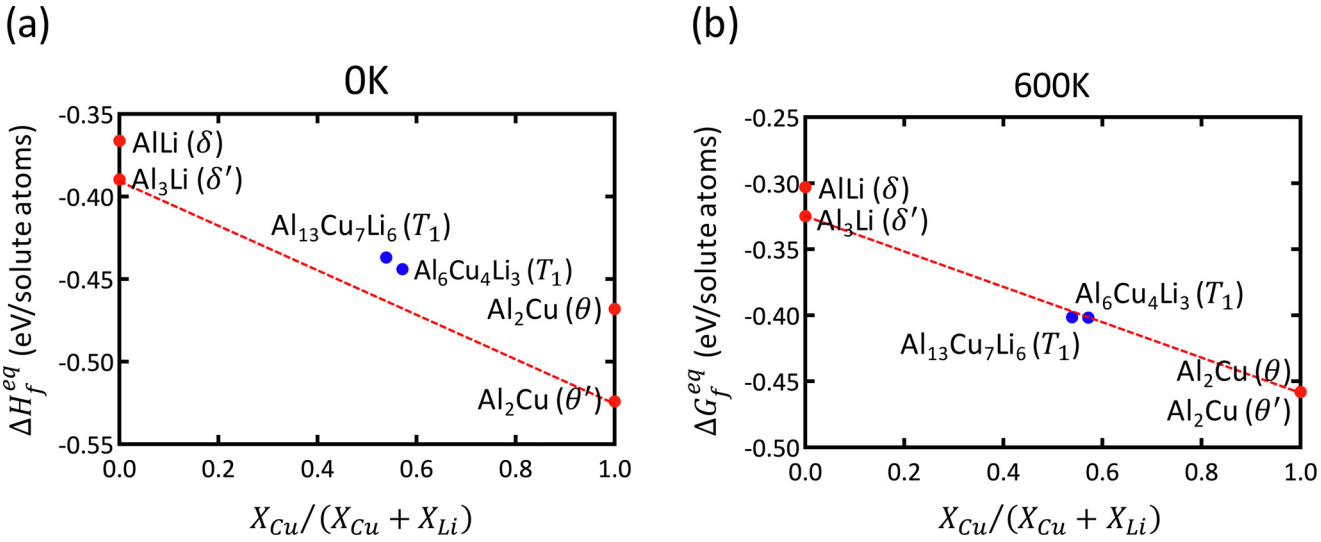

Fig. 2. Calculated formation free energies (eV/solute atom) from Eq. (1) as a function of fraction of Cu and Li at (a) 0K and (b) 600K. These energies represent the thermodynamic stability of various compounds when in equilibrium with Al matrix in the ternary Al-Cu-Li system. Blue circles indicated the previously-proposed DFT T_1 phases ($Al_6Cu_4Li_3$, $Al_{13}Cu_7Li_6$) [10]. At T=600K, the vibrational entropy stabilizes the two T_1 phases, resulting a break of the convex hull between Al_3Li (δ') and Al_2Cu (θ) at 600K. (For interpretation of the references to color in this figure legend, the reader is referred to the web version of this article.).

tions to phase stability of T_1 phase in the ternary Al-Cu-Li system. The detailed information (e.g., the formation enthalpies and entropies) is in Supplementary material. The formation free energies of Al-based compounds were computed using Eq. (1), which allows us to determine the stable phases in equilibrium with the Al matrix at 0 and 600K. In Fig. 2(b), we found that the vibrational entropy contributes stabilization of the two DFT-predicted T_1 phases at finite-temperature of 600K. The entropically stabilized T_1 phase breaks the convex hull (dotted in red), which is consistent with the experimental phase diagram. The equilibrium phase of the tetragonal (C16) structure of Al_2Cu (θ) is not the stable phase in T=0K DFT calculations as shown in Fig. 2(a). This was explained by the role of the vibrational entropies of θ and θ', which were found to be unexpectedly important for the Al_2Cu phase as proposed by Wolverton and Ozoliņš [22]. In the ternary Al-Cu-Li system at 0K, $Al_6Cu_4Li_3$ is more stable than $Al_{13}Cu_7Li_6$, however, at a temperature of 600K, $Al_{13}Cu_7Li_6$ has slightly more favorable energetics.

The multi-scale modeling from atomistic to mesoscale is a well-known design strategy in the ICME paradigms [23]. And the precipitate-matrix interfacial structure and energy are key pieces of atomistic information that can be used for mesoscale phase-field modeling of microstructural evolution. For example, the interfacial energy is an important input parameter for determining the gradient energy coefficient of the diffuse-interface approach in the phase-field method [24]. Hence, we next turn to the interfacial energy, and the concomitant requirement of determining the interfacial structure between T_1 and Al.

In order to construct an atomistic model of the T_1/Al interface, one must know the orientation relations between the precipitate and matrix crystal structures, as well as the energetically preferred termination of the precipitate phase at the interface. The

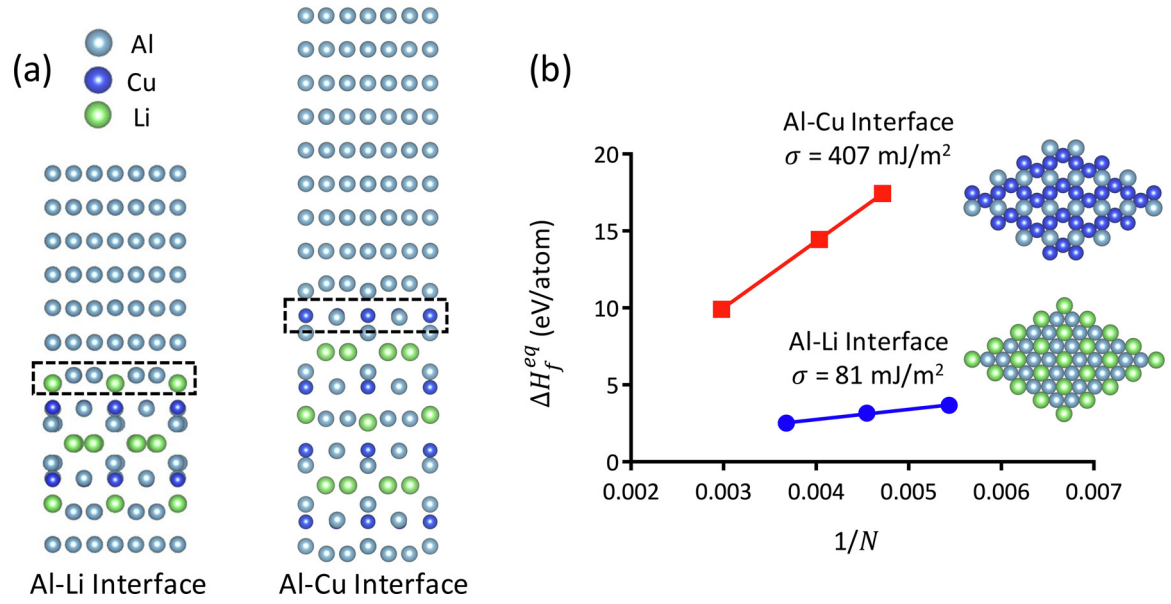

Fig. 3. (a) Relaxed atomic models for the $(0001)_{T1}/(111)_{Al}$ interfaces with different interfacial terminations (Left: Al-Li, Right: Al-Cu). (b) First-principles formation energies of N-atom super cells as a function of 1/N for the interface. The interfacial energies (σ) were extracted from the slopes by Eq. (2). The interface with Al-Cu termination has a higher slope, as such, extracted interfacial energy is higher than the interface with Al-Li termination.

T_1 precipitate forms on the {111} planes of the fcc Al matrix and have hexagonal platelet shapes [4]. According to the previous literatures, Donnadieu et al. [8] observed that the Al-Cu layers of the T_1 structure are the terminating planes of the precipitates by aberration-corrected High-Angle Annular Dark-Field Scanning Transmission Electron Microscopy (HAADF-STEM). However, Dwyer et al. [9] identified at around the same time using the same technique that the terminating precipitate layer of the interfacial structure with an Al matrix is the Al-Li corrugated layer. Based on the two experimental observations, we performed interfacial energy calculations for the two different interfacial structures to derive a low-energy structure and compute the corresponding energies by Eqs. (2) and (3).

Fig. 3(a) represents the T_1/Al interface supercells with two different terminations, Al-Cu and Al-Li layers, respectively. Our calculations found a compound interfacial energy of 81 mJ/m^2 when the nearest atoms to the interface are Al and Li. And we found that the corrugated Li layers shifted toward the Al matrix in the T_1/Al interfacial structure due to interactions with Al matrix after DFT relaxation in Fig. 3(a) (Left), consistent with two experimental observations during precipitation [9,14]. The Al-Cu terminated interface has a much higher interfacial energy of 407 mJ/m^2. The preference of Al-Li termination can be understood because the Al-Li layers are more closed-packed in two dimensions compared to the Al-Cu layers as shown in Fig. 3(b). Our finding here of Al-Li termination of the precipitate at the interface is consistent with the experimental work by Dwyer et al. [9].

Aluminum alloys are complex multi-component systems, and for example, minor solutes such as Ag and Mg are common elements in designing Al-Cu-Li alloys. The Ag and Mg solutes play an important role in stabilizing the {111} habit plane and promoting nucleation for the hexagonal structure of Ω and T_1 precipitates [25,26]. Recent experiments [13,14] show that the Ag and Mg solutes segregate to the T_1/Al interfaces, which is in contrast with Gault's finding [12] by the same experimental atom-probe tomography technique. To address this controversy and determine the solute segregation behavior at the interface, we calculated segregation energies of Ag and Mg solutes across the T_1 coherent interface.

Fig. 4(a) depicts the relaxed atomic models for solute segregation energy calculations for the T_1/Al interface determined in Fig. 3(a). The solute position with respect to the lattice plane is indicated based on the T_1/Al interface. For example, we indicate lattice planes near the interface as Al_i toward the Al matrix and T_{1i} toward the precipitate, respectively. Fig. 4(b) shows computed segregation energies of Ag and Mg solutes. A layer with a negative energy means that the solute is energetically favorable in the site compared to the Al bulk-like layer indicated as Al_b. It is shown that minor additions of Ag and Mg are thermodynamically favorable for interfacial segregations in agreement with Araullo-Peters et al. [13] and Kang et al. [14]. For example, Ag solute is favorably located on Al or Cu sites at the interface (-0.31eV/atom on T_{1i}^{Al}, and -0.18eV/atom on T_{1i-1}^{Cu}, respectively). Mg solutes prefer to locate on Li sites at interface (-0.11eV/atom on T_{1i}^{Li}). Thus, we conclude that Ag and Mg solutes segregate at the interface due to thermodynamic driving forces.

We have studied the thermodynamic stability of the bulk and interfacial structure of the T_1 precipitate in Al alloys. We refined the Li positions in the recently proposed T_1 structure. We found that the Li layers in the T_1 precipitates show a small instability and can relax away from high-symmetry positions, slightly lowering the bulk energetics. To clarify the two-phase tie line between T_1 and the Al matrix on the convex hull of Al-Cu-Li systems, we performed harmonic phonon calculations to determine the vibrational entropic stabilization. At 600K, our DFT-predicted T_1 structures are equilibrium with the Al matrix, consistent with the experimental phase diagram. We also derived a low-energy interfacial structure and energy. The low-energy interfacial structure has Al-Li atoms terminating the precipitate phase nearest to the interface. The computed lowest interfacial energy is 81mJ/m^2, which is significantly lower than that with Al-Cu termination. The minor solute segregation behaviors were investigated to resolve a discrepancy between previous observations. We found that Ag and Mg solutes were predicted to segregate at the coherent T_1/Al interface based on the segregation energy calculations across the interface. We believe that our findings will form a basis for the integrated Computational Materials Engineering (ICME) approach for designing high-strengthened Al-Cu-Li based alloys.

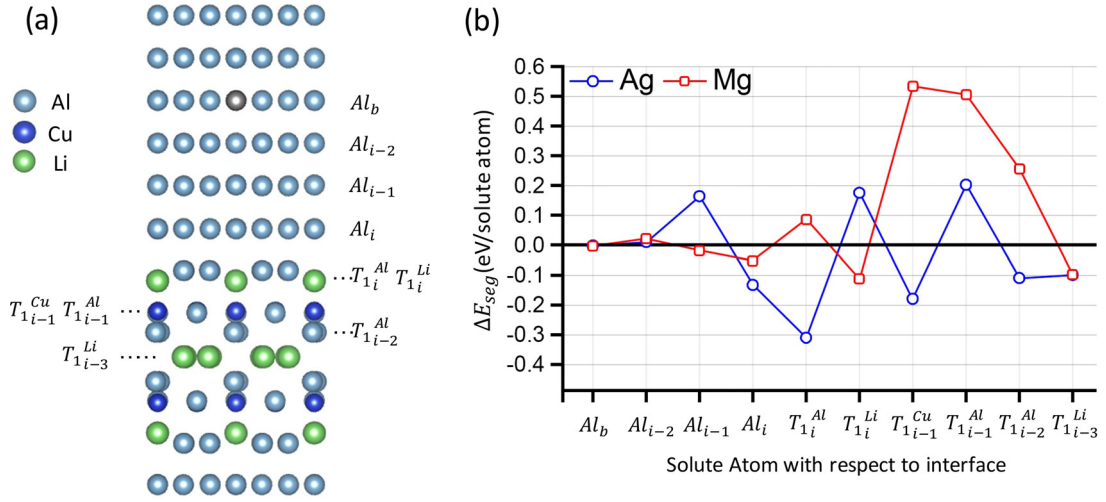

Fig. 4. (a) The relaxed atomic models for the coherent $(0001)_{T1}/(111)_{Al}$ interface used in our first-principles calculations. The black atom in the supercell illustrates a position of Ag and Mg atoms at a bulk-like site in the Al matrix. We labeled the lattice planes according to a distance from the interface plane. For example, Al_b refers to a bulk-like plane in the Al matrix; Al_i and T_{1i} represent the Al and T_1 planes adjacent to the interface. (b) Calculated Ag and Mg solute segregation energies as a function of distance from the coherent interface. The blue points represent Ag solute and red points represent Mg solute at the interface, respectively. The sites that have a sign convention of are energetically favorable compared to Al bulk-like sites in the matrix.

Declaration of Competing Interest

The authors declare that they have no known competing financial interests or personal relationships that could have appeared to influence the work reported in this paper.

Acknowledgement

This work has supported by the National Research Foundation of Korea (NRF) grant funded by the Korea government (MSIT) (No. 2021R1C1C1012756). B. N and K. K. acknowledge the support from Inha University under Grant No. 62582-01. B. C. Z. acknowledges support from Beijing International Aeronautical Materials Corp. (BIAM). C. W. was supported by The Center for Hierarchical Materials Design (CHiMaD), Dept. of Commerce, NIST under award number 70NANB14H012.

Supplementary materials

Supplementary material associated with this article can be found, in the online version, at doi:10.1016/j.scriptamat.2021.114009.

References

[1] F.W. Gayle, F.H. Heubaum, J.R. Pickens, Scr. Metall. Mater. 24 (1) (1990) 79–84.
[2] E.A. Starke Jr., J.T. Staley, Prog. Aerosp. Sci. 32 (2) (1996) 131–172.
[3] E.J. Lavernia, T.S. Srivatsan, F.A. Mohamed, J. Mater. Sci. 25 (2) (1990) 1137–1158.
[4] C.P. Blankenship, E.A. Starke, Acta Metall. Mater. 42 (3) (1994) 845–855.
[5] J.C. Huang, A.J. Ardell, Mater. Sci. Technol. 3 (3) (1987) 13.
[6] J.M. Howe, J. Lee, A.K. Vasudevan, Met. Mater. Trans. A 19A (1988) 2911–2920.
[7] S. Van Smaalen, A. Meetsma, J.L. De Boer, P.M. Bronsveld, J. Solid State Chem. 85 (2) (1990) 293–298.
[8] P. Donnadieu, Y. Shao, F. De Geuser, G.A. Botton, S. Lazar, M. Cheynet, M. de Boissieu, A. Deschamps, Acta Mater. 59 (2) (2011) 462–472.
[9] C. Dwyer, M. Weyland, L.Y. Chang, B.C. Muddle, Appl. Phys. Lett. 98 (20) (2011) 201909.
[10] K. Kim, B.-C. Zhou, C. Wolverton, Acta Mater. 145 (2018) 337–346.
[11] K. Kim, P.W. Voorhees, Acta Mater. 152 (2018) 327–337.
[12] B. Gault, F. de Geuser, L. Bourgeois, B.M. Gabble, S.P. Ringer, B.C. Muddle, Ultramicroscopy 111 (6) (2011) 683–689.
[13] V. Araullo-Peters, B. Gault, F.d. Geuser, A. Deschamps, J.M. Cairney, Acta Mater. 66 (2014) 199–208.
[14] S.J. Kang, T.-H. Kim, C.-W. Yang, J.I. Lee, E.S. Park, T.W. Noh, M. Kim, Scr. Mater. 109 (2015) 68–71.
[15] G. Kresse, J. Furthmüller, Phys. Rev. B 54 (16) (1996) 11169–11186.
[16] G. Kresse, D. Joubert, Phys. Rev. B 59 (3) (1999) 1758–1775.
[17] J.P. Perdew, K. Burke, M. Ernzerhof, Phys. Rev. Lett. 77 (18) (1996) 3865–3868.
[18] A. Togo, I. Tanaka, Scr. Mater. 108 (2015) 1–5.
[19] K. Kim, A. Bobel, V. Brajuskovic, B.-C. Zhou, M. Walker, G.B. Olson, C. Wolverton, Acta Mater. 154 (2018) 207–219.
[20] V. Vaithyanathan, C. Wolverton, L.Q. Chen, Acta Mater. 52 (10) (2004) 2973–2987.
[21] K. Kim, B.-C. Zhou, C. Wolverton, Scr. Mater. 159 (2019) 99–103.
[22] C. Wolverton, V. Ozoliņš, Phys. Rev. Lett. 86 (24) (2001) 5518.
[23] J. Allison, M. Li, C. Wolverton, X. Su, JOM 58 (11) (2006) 28–35.
[24] K. Kim, A. Roy, M.P. Gururajan, C. Wolverton, P.W. Voorhees, Acta Mater. 140 (2017) 344–354 (Supplement C).
[25] L. Reich, M. Murayama, K. Hono, Acta Mater. 46 (17) (1998) 6053–6062.
[26] T. Honma, S. Yanagita, K. Hono, Y. Nagai, M. Hasegawa, Acta Mater. 52 (7) (2004) 1997–2003.